Smart Metal–Polymer Bionanocomposites as Omnidirectional Plasmonic Black Absorber Formed by Nanofluid Filtration

Mady Elbahri, Shahin Homaeigohar, Ramzy Abdelaziz, Tianhe Dai, Rania Khalil, and Ahnaf Usman Zillohu*

The first smart plasmonic absorber based on metal-polymer bionanocomposites performing via conformational changes of the biological functional agent, i.e., a protein, is introduced. Such a progress is done through bridging the gaps between nanofluid filtration, plasmonics, and bioswitching. Initially, a biofunctionalized nanofibrous membrane is developed that could filter out metal nanoparticles (<100 nm) from an aqueous stream with a high separation efficiency (97%). This approach brings about a breakthrough in applicability of the macroporous nanofibrous membranes for rejection of suspended nanosolids and extends the application area beyond microfiltration (MF) to ultrafiltration (UF). This operative filtration in the next step leads to a novel synthesis route for plasmonic materials as formation of a smart free-standing metal–polymer bionanocomposite able to act as an omnidirectional black absorber.

1. Introduction

Bionanocomposites as a novel group of nanostructured hybrid materials possess a combination of biopolymers and nanoscale inorganic solids.[1,2] The biological component of the bionanohybrid not only brings about a biocompatibility and environmentally friendly nature to the nanohybrid but also stabilizes the inorganic solid.[3,4] Moreover, the stimulus-responsive behaviour of the biological component would provide the nanohybrid with a smart functionality.[5,6]

Prof. M. Elbahri, Dr. Sh. Homaeigohar, Dr. T. Dai, A. U. Zillohu
Helmholtz-Zentrum Geesthacht
Institute of Polymer Research
Nanochemistry and Nanoengineering
Max-Planck-Str.1, 21502, Geesthacht, Germany
E-mail: mady.elbahri@hzg.de
Prof. M. Elbahri, R. Abdelaziz, Dr. R. Khalil
Faculty of Engineering
University of Kiel
Institute for Materials Science
Nanochemistry and Nanoengineering
Kaiserstrasse 2,24143 Kiel, Germany
Dr. R. Khalil
Department of Physics
Faculty of Science
Zagazig University
Zagazig 44519, Egypt

DOI: 10.1002/adfm.201200768

As the second constituent, the inorganic nanocomponents, e.g., metal nanoparticles, show promising properties in terms of optical, magnetic, etc.[7] Exhibiting optimum structural and functional properties arose from either the biological or inorganic moieties, these biohybrid materials have been envisaged suitable for a diverse range of advanced applications such as plasmonics.[1,6,8]

Plasmonics is a rapidly growing field on the cutting edge of optical sciences, photonics and nanotechnology. It aims to exploit the unique optical properties of metallic nanostructures to enable routing and active manipulation of light at the nanoscale thereby creating fascinating optical devices such as plasmonic absorbers. Nowadays, designing plasmonic black absorbers for a wide range of applications, e.g., photodetectors,[9–11] microbolometers[12] and thermophotovoltaic solar energy convertors,[13–17] is highly demanded.

Even though designing a plasmonic absorber at visible frequencies is still a challenge, among the techniques used for this purpose; grating structured system, perforated metallic film and metamaterial[18–20] could somewhat approach to such a desire. However, all the mentioned methods are costly and suffer from the lack of flexibility and the absorbance obtained is limited to a narrow range of frequencies. Advantageous over the previous techniques, recently we introduced a broadband plasmonic absorber with almost 100% absorbance spanning the broad area of frequencies from UV to NIR. This plasmonic absorber was made through sputter coating of a metal film with a metal/dielectric nanocomposite.[21] As one step ahead to simplify the fabrication process and naturally to minimize the costs, as the forthcoming study, we introduce devising a smart black absorber based on free-standing nanocomposites in a fiber mat form.

While the fabrication of such nanocomposites is crucially limited by the strong tendency of nanoparticles to aggregate on the polymeric surface.[22–25] Here, as a novel strategy, we developed an operative fabrication method for plasmonic bionanohybrids based on a filtration process. To do so, a membrane composed of electrospun nanofibers functionalized by a protein ligand is utilized. Separation of metal nanoparticles from the respective aqueous suspension by this nanofibrous membrane would give rise to formation of a bionanohybrid. Such a performance implies the applicability of the membrane for water treatment by itself as well.

Electrospun nanofibrous membranes (ENMs) compared to their conventional counterparts are more porous and possess an interconnected porous structure thereby show an extraordinary permeability giving rise to a low energy consumption. Yet, such membranes suffer from low mechanical stability also hydrophobicity and are usually as low selective as microfiltration (MF) membranes. As a shortcoming for our fabrication approach, these membranes owing to their micro-sized pores are able to capture only coarse suspended solids rather than nanosized substances, e.g., metal nanoparticles.[26–31] The promising solution to preserve the high permeability of the nanofibrous membranes while optimizing their retention efficiency as prerequisites of an operative nanofluid filtration subsequently an energy/cost efficient fabrication of a plasmonic nanohybrid is biofunctionalization of the nanofibers.

Our filtration based fabrication method of the bionanocomposite is assumed to benefit the unique smart conformational and structural properties of the biofunctional agent with a novel dual role as: 1) the capturer of metallic nanoparticles and 2) the structural tuner of the first smart omnidirectional broadband black absorber with almost 100% absorbance spanning the visible frequencies.

To the best of our knowledge, filtration using macroporous electrospun nanofibrous mats to capture nanoparticles and adopting this approach as a facile route to fabricate a tunable nanocomposite black absorber has never been reported. Indeed, through this study we bridge the gap between several fields including filtration, plasmonics and bioswitching.

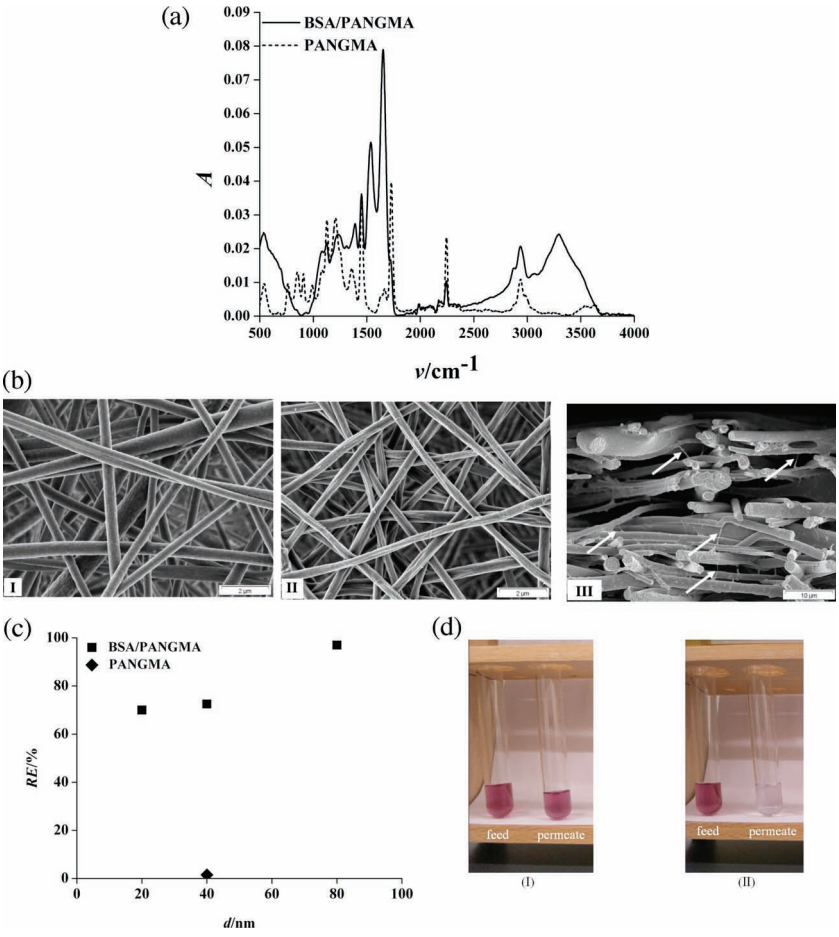

Figure 1. a) ATR-FTIR spectra of the PANGMA ENMs before and after BSA immobilization. *A* and *ν* represent absorbance and wavenumber, respectively. b) SEM images of the PANGMA nanofibers as neat (I: overview) and BSA immobilized (II: overview and III: cross-section; arrows indicate the BSA induced cross linking of the nanofibers). c) Extraordinary nanofluid filterability after biofunctionalization proved via UV-Vis measurements (d at the x-axis represents the nanoparticle diameter). d) Extraordinary nanofluid filterability after biofunctionalization proved via visual comparisons between the feed and permeated samples through the neat (I) and BSA/PANGMA ENMs (II).

2. Results and Discussion

As the current study, we functionalized poly(acrylonitrile-*co*-glycidyl methacrylate) (PANGMA) nanofibers through surface immobilization with Bovine Serum Albumin (BSA). BSA acting as the capturer component is a cheap serum albumin protein, widely used in numerous biochemical applications. Moreover, PANGMA as a new polymeric material is a copolymer of acrylonitrile (AN) and glycidyl methacrylate (GMA).[32] This polymer possesses a suitable chemical stability induced by the strong backbone of polyacrylonitrile. Moreover, the presence of a free and active epoxy group on GMA could lead to a high functionality thereby the feasibility of a variety of activation/coupling chemistries for the covalent binding of capturers. In the current study, the nanofibers are functionalized based on the extremely simple and conventional epoxy-amino reaction between the amine groups on BSA and epoxy groups on PANGMA.[32,33]

Functionalization mechanism of PANGMA is based on ring opening of the epoxide groups of its GMA part when attacked by amine containing BSA. The result of such a reaction is formation of the secondary amine and hydroxyl groups. Such an assumption is proved by the surface chemical analysis results shown in **Figure 1**a. Successful reaction between primary amine groups of BSA and epoxides of PANGMA is emphasized by vanishing the characteristic peak of epoxy group appearing at 908 cm^{-1} for the neat nanofibers. In addition, the peaks emerging at 1650 cm^{-1} and 1530 cm^{-1} are the vibration peaks of amide I and amide II groups in BSA molecules. The peaks at 3300 and 3600 cm^{-1} are related to the secondary amine and hydroxyl groups, respectively, generated during the opening of the epoxy group by the primary amine groups of BSA.[34,35]

Possessing lots of primary amine groups, BSA can also react with two adjacent PANGMA nanofibers leading to a cross linked structure. While, the overview pictures obtained by scanning electron microscopy (SEM) (Figures 1bI,II) reveal no

significant difference in term of porosity between the neat and functionalized nanofibrous mats, the cross sectional image of the latter group (Figure 1bIII) clearly indicates that the submicrometer fibers are interconnected by nanometer protein wires. This behaviour was not observed for the neat membrane. Such an increase of the netting points of the web and interfiber bondings are expected to strengthen the membrane.[36,37] This effect is intensified by crosslinking of the PANGMA molecules inside the nanofibers while functionalization. Indeed, the biofunctionalization giving rise to inter/intrafiber bondings leads to a significantly higher mechanical stability in terms of elastic modulus (E) and tensile strength (σ) as 194% and 300% increase, respectively, compared to those of the neat PANGMA ENM. A mechanically strong nanofibrous membrane can resist against pore collapse while filtration subsequently possesses a longer life span and lower energy consumption.[38] A water filtration test under a 1 bar pressure, clearly showed that the mechanically stronger BSA/PANGMA ENM is much more permeable (~45 kl h^{-1} m^{-2}) than its neat counterpart. Yet, some part of this higher permeability is attributed to the superhydrophilicity of the functionalized membranes arose from emergence of the secondary functional groups which could lower the filtration resistance. As proved via a water contact angle measurement, while the neat membrane showed a water contact angle of 130°, this value for the biofunctionalized one was only 5° implying their hydrophobicity and superhydrophilicity, respectively.

Applicability of electrospun nanofibrous membranes is significantly promoted when they are able to perform beyond a MF membrane capturing not only coarse suspended solids but also nanosolids much smaller than the pore size. Here, we aim to show that functionalization through BSA immobilization, brings about a highly selective energy saving UF ENM able to capture metal nanoparticles. As a proof of the concept, gold (Au) nanoparticles containing aqueous suspensions were filtered. The nanoparticles used in the model feed system had a size of 20, 40 and 80 nm in the range of UF.

Retention ability of the BSA/PANGMA ENMs for the gold nanoparticles is demonstrated in Figure 1c. As the control experiment to compare the filtration performance of the functionalized PANGMA ENM with its neat counterpart, the suspension containing 40 nm Au nanoparticles was randomly selected. While the neat PANGMA ENM is able to reject a negligible part (1.5%) of the 40 nm Au nanoparticles, the biofunctionalized ENM rejects 72.5% of the nanoparticles of the same size. Visual inspection of the feed and permeate samples clearly reveals the high retention ability of the BSA/PANGMA ENM compared to its neat counterpart. As seen in Figure 1d, color intensity of the feed sample drastically decreases after permeation through the biofunctionalized ENM.

The retention efficiency for 80 nm Au nanoparticles is even more as high as 97%, whereas this value for the 20 nm nanoparticles reduces to 70%, still high and promising. In addition to such an extraordinary retention efficiency, the permeate flux recorded when filtration of 80 nm Au suspension, was also considerable as high as 9000 l $h^{-1}m^{-2}$ much higher than that reported for conventional micro/ultrafiltration membranes.[27] Noteworthy, there was no major feed pressure while filtration and the experiment was performed under the atmospheric pressure implying a very low energy consumption.

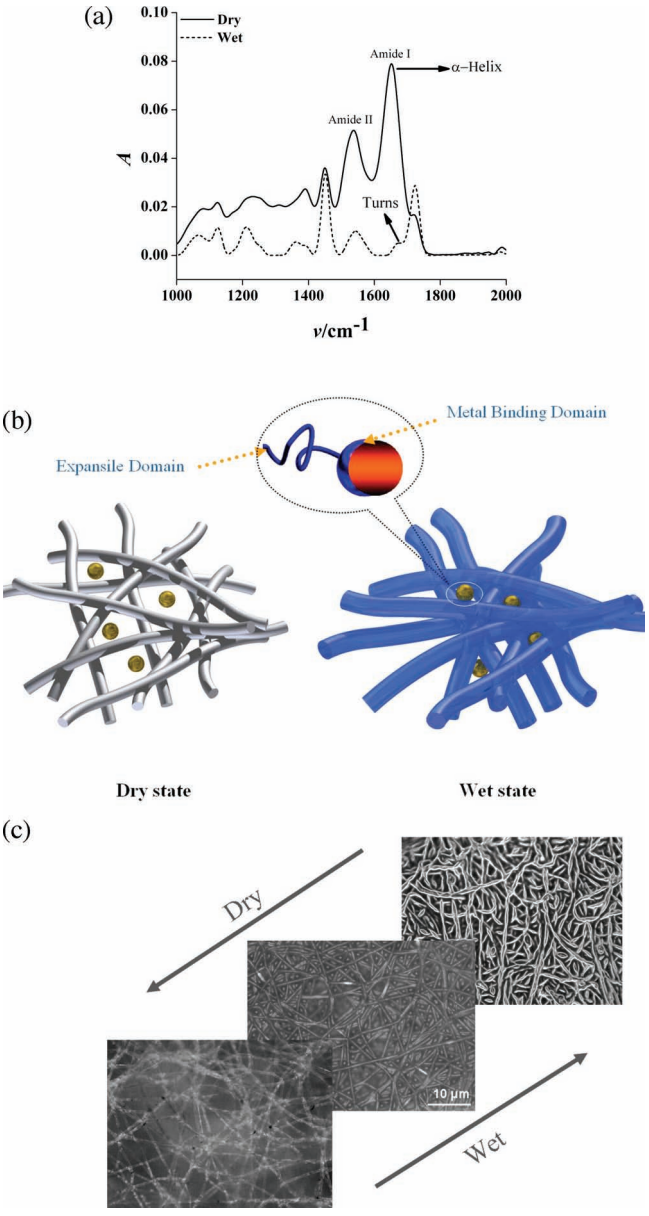

Figure 2. a) ATR-FTIR spectra of the BSA/PANGMA ENMs as dry (the solid upper line) and wet (the dashed lower line). b) The sketch illustrates how the swollen functionalized nanofibers capture the nanoparticles. c) The optical images show morphological change of the membrane and the reversible swelling of the functionalized nanofibers in wet and dry states implying a smart performing membrane.

As shown in **Figure 2**a–c, the reason for such a high retention efficiency by the BSA/PANGMA ENMs should be sought in the conformational change of the immobilized BSA. Indeed, the configuration of BSA as folded or unfolded would play a governing role in its capturing ability of nanoparticles. In the folded state i.e. "α- helix", the tryptophan and cysteine residue groups which are able to interact with metal nanoparticles are mostly located within the protein structure and not exposed.[39] Furthermore, owing to the strong internal hydrogen bonds between the peptide groups, other functional

groups such as amine based groups are less available on the surface as well. However, a conformational change during the filtration stimulates the unfolding of BSA as β- turn, thereby emergence of these active groups on the surface capable ideally to capture the nanopartciles.

This alteration is traceable through ATR-FTIR measurements (Figure 2a) as replacement of the bands assigned to α- helix secondary structure of BSA (1650–1658 cm^{-1}) predominated in dry state with those of turns (1666–1673 cm^{-1})[40,41] in wet state. As a result, previously buried peptide bonds such as those appeared in wet state at 1210 and 1721 cm^{-1} (corresponding to C–N and C=O) and amino acid side chains are exposed and can interact with the aqueous environment. Such a transformation leads to binding considerably more water[42] giving rise to a swollen structure. From one hand, expansion of the protein on the surface of the nanofibers makes a smaller pore size and more steric hindrance by growing nanofibers (Figure 2b,c). On the other hand, upon the conformational change the functional protein groups become exposed on the surface. These binding groups could capture the nanoparticles and stabilize them by strong protein- metal nanoparticle interactions such as ionic interaction, hydrogen bonding, Van der Waals and hydrophilic interactions,[43–45] thus Au nanoparticles stick to BSA protein. Combination of these effects reminds us the hunting behaviour of a carnivorous plant and results in a significantly high retention efficiency for the membrane being studied. This retention ability is intensified as soon as adsorption of the first batch of metal nanoparticles to the functionalized nanofibers leading to gradual change of the surface color as well. Interestingly, as long as the filtration goes on, i.e., after the 2nd to 3rd cycle, more nanoparticles are adsorbed onto the nanofibers thereby the surface color becomes darker and finally shifts to black.

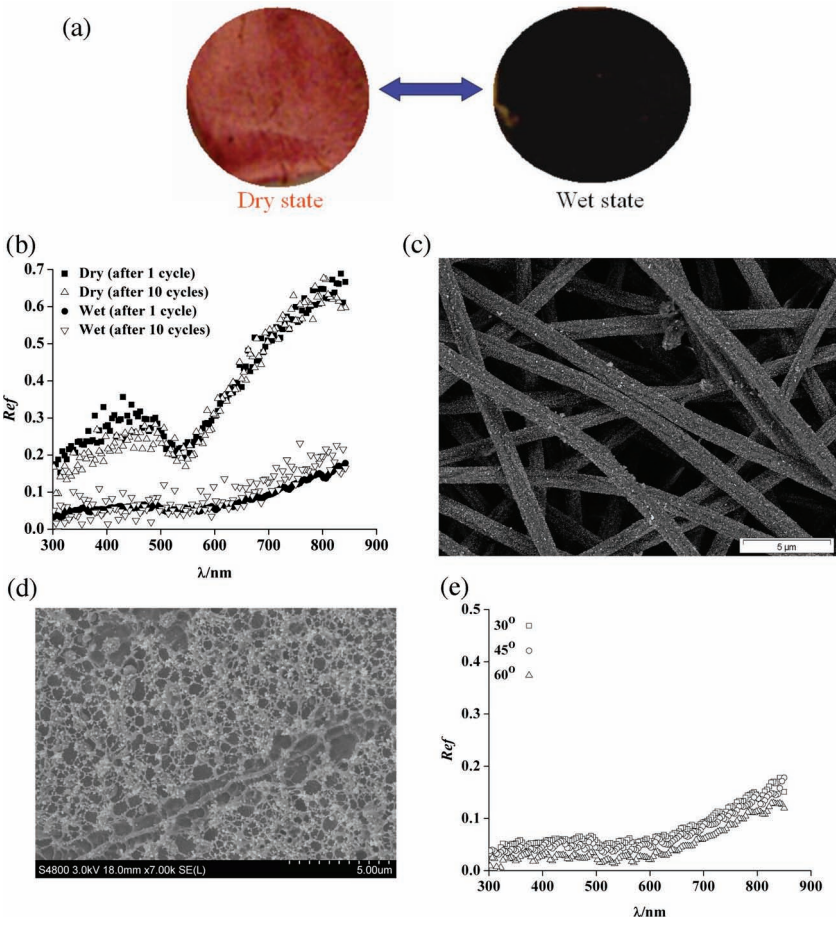

Figure 3. a) Tunable coloration of the surface of the membrane at dry (red) and wet (black) states. b) The reflection spectra of the nanocomposite in dry and wet (completely water soaked) states. Ref and λ represent reflection and wavelength, respectively. c) Formation of a bionanohybrid structure through adsorption of Au nanoparticles onto the BSA/PANGMA nanofibers. d) Cryo-SEM image showing the surface of the wetted (water soaked) membrane. e) The reflection spectra of the black absorber nanocomposite measured at different light incidence angles.

Biofunctionalization not only could revolutionize filtration performance of an ENM but also it can equip the membrane to some further abilities e.g. creating plasmonic nanocomposites. For instance, the Au nanoparticle/BSA/PANGMA nanofibrous membrane as dried possesses a reddish color attributed to the gold nanoparticles adsorbed on the membrane's surface. The intensity of the color strongly depends on the amount of the nanoparticles adsorbed and indirectly on the filtration duration. However, when the membrane is soaked in water to remove the weakly adsorbed i.e. "non-captured" nanoparticles, the membrane's color becomes black. Drying the membrane again leads to returning the red color. We repeated this process for ten cycles with a fully repeatability. Such a performance certifies the applicability of our smart bionanocomposite in development of switchable plasmonic materials.

The influence of the water-induced structural changes on the collective optical properties of the nanocomposites is shown in **Figure 3**a. As observed in this figure, there is a tunable coloration of the sample from red to black in dry and wet states, respectively. UV-Vis measurements support the naked eyes observation. Figure 3b shows the reflection spectra of the nanocomposite in dry and wet states at the start and after 10 cycles of repetitions. Obviously, depending on the hydration states, the color of the membrane changes from red, recognized by a reflection dip at 537 nm, to black with vanishing reflections in the visible ranges. More specifically, the reflection measurement of the black absorber shows wide resonances broadly spanning the spectral range from NUV to NIR with an alleviated reflection and a complete absorption of nearly 100%.

Figure 3c clearly confirms that the adsorption of tiny gold nanoparticles onto the functionalized nanofibers gives rise to development of the red plasmonic nanocomposites. The black state is associated with the tunable conformation which was investigated by cryo-SEM. As seen in Figure 3d, the black hybrid could be resembled to a swollen open porous nanostructured

foam. Formation of the porous structure reveals a phase separation in the fully hydrated membrane. Indeed the fabricated bionanocomposite is characterized by the presence of hydrophilic domains embedded in/ attached on the hydrophobic polymer matrix. The hydrophobic domains apply considerable constraints upon the hydrophilic amorphous regions, restricting their swelling by inhibiting deformation parallel to their surfaces. Owing to the limited segmental mobility, an osmotic pressure is developed in the matrix which can lead to the formation of voids. Expansion of the voids is opposed by the vitrification of the polymer-rich matrix surrounding them. Thus, the balance between the two opposite forces gives rise to the formation of porous structures decorated by the nanoparticles in a nanoaggregation- like fashion.

Because of the nanoaggregation, there is a diversity of structures which reinforce the localized plasmon excitations and strongly couple them in a broad spectral range.[46–50] It is well known that in the case of closely spaced nanoparticles (near percolation), strong near field coupling occurs and energy can be efficiently trapped.[51] The light trapping is intensified when the incident light is diffracted or scattered by the accumulated nanoparticles. Hereby, the light is encouraged to enter into the structure rather than to reflect back. Utilization of a layer thick enough to prevent the light from passing through and able to trap the energy thereby to suppress the reflection, will obstruct the incident light and make the device as a black absorber.

However, it is not yet clear if our porous metal-polymer nanocomposite possessing the pores as large as the wavelength of the incident radiation in visible frequency, could behave as an "electromagnetic black body".

The theoretical work by Narimanov and Kildishev[52] on an optical metamaterials based omnidirectional light absorber shows that all the optical waves hitting the concentrator[53] are trapped and absorbed. The proposed hybrid device is composed of non-resonant and resonant metamaterial structures (spirally or a cylinder), which can trap and absorb electromagnetic waves coming from all directions without any reflections due to the local control of electromagnetic fields. Similarly, our metal polymer bionanocomposite black absorber is not sensitive to the incidence angle of the light. Figure 3e, illustrates that there is no considerable angular dependence of the reflection measurement of the sample ranging from 30° to 60° on corresponding reflectivity of the structure in all the incidence angels. However, our finding needs further experiments currently being in progress in our laboratory. On the whole, to the best of our knowledge our work is the first report on design of a black plasmonic absorber at the visible frequency using free-standing nanocomposites via a nanofluid filtration process. Noteworthy, besides creation of the black absorber, the membrane could be used for a novel water treatment i.e., separation of metal nanoparticles from waste water streams as well. For example, silver nanoparticles are frequently used in consumer products (e.g., in socks to inhibit odor-causing bacteria) due to their promising potential of bactericidal. However, recent studies have shown that such nanoparticles in case release can kill also benign bacteria being used in removal of ammonia from wastewater treatment systems.[54] Hence, there is a necessity in removal of metal nanoparticles released in waste water streams. As proved through the current study, our novel membrane showed such a potential.

3. Conclusion

In summary, by developing a novel bio assisted nanofluid filtration route, a smart perfect plasmonic black absorber based on a metal-polymer bionanocomposite is designed and introduced for the first time. Such a progress was done through bridging the gaps between nanofluid filtration, plasmonics and bioswitching. Initially, a biofunctionalized nanofibrous membrane was developed that could filter out metal nanoparticles (<100 nm) from an aqueous stream with a high separation efficiency (97%), an optimum permeability, mechanical stability also wettability. This approach brings about a breakthrough in applicability of the macroporous nanofibrous membranes for rejection of suspended nanosolids and extends the application area beyond MF to UF. This operative filtration in next step leads to a novel synthesis route for plasmonic materials as formation of a smart free-standing metal-polymer bionanocomposite able to act as a black absorber.

4. Experimental Section

Materials: Poly(acrylonitrile-*co*-glycidyl methacrylate) (PANGMA) was synthesized by Helmholtz-Zentrum Geesthacht (HZG) (previously GKSS Forschungszentrum GmbH)[55] with a molecular weight (M_n) of ca. 100 000 g mol^{-1} and GMA content of 13 mol%. Bovine Serum Albumin (BSA) (dried powder) and Phosphate Buffered Saline (PBS) were purchased from Sigma-Aldrich Co. *N,N*-dimethylformamide (DMF) and methanol were purchased from Merck KGaA. All the chemicals were directly used without purification.

While, the Au nanoparticles of 20 nm (Gold colloid G1652, G1402) were purchased from Sigma-Aldrich Co. and used without further purification, those of 40 and 80 nm were made using sodium citrate reduction method reported by Wang.[56]

Preparation of PANGMA ENMs by Electrospinning: Briefly, prepared PANGMA solution (20 wt%) in *N,N*-dimethylformamide (DMF) was fed with a constant rate of 1.1 ml h^{-1} into a needle by using a syringe pump (Harvard Apparatus, USA). By applying a voltage of 15–20 kV (Heinzinger Electronic GmbH, Germany) electrospinning was done on an Aluminum (Al) foil located 25 cm above the needle tip for 4 h. After all, the nanofibrous mat was peeled off from Al foil and dried under vacuum at 30 °C for 24 h to remove the residual solvent.

BSA Immobilization: PANGMA ENMs were immersed into the BSA/PBS buffer (5 mg ml^{-1}) (pH 6.8) and the mixture was moderately shaken at 55 °C for 24 h. Then, the membranes were taken out and washed several times by PBS buffer (pH 6.8) to remove all the unbound BSA. Finally, the BSA immobilized PANGMA ENMs were carefully washed with deionized water and dried under vacuum at 30 °C for 24 h.

Morphological and Structural Characterizations: The morphology of the PANGMA ENMs was observed with a scanning electron microscope (LEO Gemini 1550 VP, Zeiss). The wet sample was investigated by a Scanning Electron Microscope Hitachi S 4800 equipped with Gatan Alto 2500 Cryo Preparation System.

Optical measurements of the dry and wet composite samples were done using a UV-Vis/IR spectrometer (Lambda 900).

Chemical surface analysis of both the neat and BSA immobilized PANGMA ENMs was performed by Fourier Transform Infra Red Spectrometry (FTIR). Attenuated total reflection Fourier transform infrared (ATR-FTIR) spectra were recorded using a Bruker Equinox 55 spectrometer.

Mechanical Characterization (Tensile Test): The tensile mechanical properties of the PANGMA ENMs were characterized by a tensile machine (Zwick/Roell Z020-20KN, Germany) equipped with a 20-N load-cell at ambient temperature. The cross-head speed was 2 mm min^{-1} and the gauge length was 20 mm. The reported tensile moduli, tensile strengths and elongations represented average results of 10 tests.

Wettability Characterization: Wettability of the PANGMA ENMs was characterized through water contact angle measurement, using a contact angle analysis system (Kruess DSA 100, Germany). A 5 µl droplet was dispensed on the membrane and the resultant angle was measured.

Water Permeability Analysis: Water Permeability of the PANGMA ENMs as neat and functionalized was evaluated through a water flux measurement using a custom-built set-up (shown in ref. [57]). The circular membranes (d = 20 mm) were stamped out and placed over a poly(*p*-phenylene sulfide) (PPS) technical nonwoven support layer. 300 ml water was passed through the membranes under a 1 bar applied pressure. The water flux was calculated by Equation (1):

$$J = \frac{Q}{A\Delta t} \quad (1)$$

where J is the water flux (l $h^{-1}m^{-2}$), Q is the permeated volume of water (l), A is the effective area of the ENMs (m^2), and Δt is the sampling time (h). All the flux measurements were repeated three times.

Retention Test with Metal Nanoparticle Containing Aqueous Suspension: The retention capability of the neat and biofunctionalized PANGMA ENMs was determined using aqueous suspensions containing gold nanoparticles with different average particle sizes including 20, 40 and 80 nm. The suspensions (20 ml) were passed through the membranes with the same configuration as those in the water permeability test. This process was done as three successive cycles i.e., the first permeate was used as the second feed and the second permeate as the third feed. Meanwhile, the permeation time was recorded. Noteworthy, the filtration was performed under a negligible hydrostatical pressure i.e., no considerable feed pressure.

Already assessing gold nanoparticle aqueous suspension calibration curve, the concentrations of gold nanoparticles in the original feed and permeate were determined by UV-Vis spectroscopy (HITACHI U-3000, HITACHI). The retention efficiency (RE) was determined according to Equation (2):

$$RE = \left(1 - \frac{C_{permeate}}{C_{feed}}\right) \times 100\% \quad (2)$$

where $C_{permeate}$ and C_{feed} are the permeate and feed concentrations, respectively.

Acknowledgements

M.E. thanks the initiative and networking fund of the Helmholtz Associations for providing the financial base of the start-up of his research group. The authors would like to acknowledge Prof. Dr. Gorb for Cryo-SEM imaging of the samples, Stefan Rehders for drawing the 3D sketch of the membranes, Kristian Bühr for design of water flux measurement set-up, Heinrich Böttcher for tensile tests, and Karen-Marita Prause for SEM measurements.

Received: March 19, 2012
Revised: May 22, 2012
Published online: July 10, 2012

[1] M. Darder, P. Aranda, E. Ruiz-Hitzky, *Adv. Mater.* **2007**, *19*, 1309.
[2] E. R. Ruiz-Hitzky, M. Darder, P. Aranda, *J.Mater. Chem.* **2005**, *15*, 3650.
[3] C. Mao, D. J. Solis, B. D. Reiss, S. T. Kottmann, R. Y. Sweeney, A. Hayhurst, G. Georgiou, B. Iverson, A. M. Belcher, *Science* **2004**, *303*, 213.
[4] R. Brayner, M. J. Vaulay, F. Fievet, T. Coradin, *Chem. Mater.* **2007**, *19*, 1190.
[5] D. Roy, J. N. Cambre, B. S. Sumerlin, *Prog. Polym. Sci.* **2010**, *35*, 278.
[6] C. Aime, I. B. Rietveld, T. Coradin, *Chem. Phys. Lett.* **2011**, *505*, 37.
[7] F. Faupel, V. Zaporojtchenko, T. Strunskus, M. Elbahri, *Adv. Eng. Mater.* **2010**, *12*, 1177.
[8] M. Alsawafta, S. Badilescu, V.-V. Truong, M. Packirisamy, *Nanotechnology* **2012**, *23*, 065305.
[9] Y. Ahn, J. Dunning, J. Park, *Nano Lett.* **2005**, *5*, 1367.
[10] Y. Gu, E. S. Kwak, J. L. Lensch, J. E. Allen, T. W. Odom, L. J. Lauhon, *Appl. Phys. Lett.* **2005**, *87*, 043111.
[11] O. Hayden, R. Agarwal, C. M. Lieber, *Nat. Mater.* **2006**, *5*, 352.
[12] P. L. Richards, *J.Appl. Phys.* **1994**, *76*, 1.
[13] T. J. Coutts, *Renew. Sustain. Energy Rev.* **1999**, *3*, 77.
[14] S. Y. Lin, J. Moreno, J. G. Fleming, *Appl. Phys. Lett.* **2003**, *83*, 380.
[15] H. Sai, H. Yugami, *Appl. Phys. Lett.* **2004**, *85*, 3399.
[16] M. Law, L. E. Greene, J. C. Johnson, R. Saykally, P. Yang, *Nat. Mater.* **2005**, *4*, 455.
[17] B. Tian, X. L. Zheng, T. J. Kempa, Y. Fang, N. F. Yu, G. H. Yu, J. L. Huang, C. M. Lieber, *Nature* **2007**, *449*, 885.
[18] V. G. Kravets, F. Schedin, A. N. Grigorenko, *Phys. Rev. B* **2008**, *78*.
[19] H. Tao, C. M. Bingham, A. C. Strikwerda, D. Pilon, D. Shrekenhamer, N. I. Landy, K. Fan, X. Zhang, W. J. Padilla, R. D. Averitt, *Phys. Rev. B* **2008**, *78*.
[20] N. Liu, M. Mesch, T. Weiss, M. Hentschel, H. Giessen, *Nano Lett.* **2010**, *10*, 2342.
[21] M. K. Hedayati, M. Javaherirahim, B. Mozooni, R. Abdelaziz, A. Tavassolizadeh, V. S. K. Chakravadhanula, V. Zaporojtchenko, T. Strunkus, F. Faupel, M. Elbahri, *Adv. Mater.* **2011**, *23*, 5410.
[22] Y. Wang, Q. Yang, G. Shan, C. Wang, J. Du, S. Wang, Y. Li, X. Chen, X. Jing, Y. Wei, *Mater. Lett.* **2005**, *59*, 3046.
[23] H. K. Lee, E. H. Jeong, C. K. Baek, J. H. Youk, *Mater. Lett.* **2005**, *59*, 2977.
[24] I. Hayakawa, Y. Iwamoto, K. Kikuta, S. Hirano, *Sens. Actuators B* **2000**, *62*, 55.
[25] Z. Zhang, M. Han, *J. Mater. Chem.* **2003**, *13*, 641.
[26] V. Thavasi, G. Singh, S. Ramakrishna, *Energy Environ. Sci.* **2008**, *1*, 205.
[27] S. Ramakrishna, R. Jose, P. S. Archana, A. S. Nair, R. Balamurugan, J. Venugopal, W. E. Teo, *J. Mater. Sci.* **2010**, *45*, 6283.
[28] S. Sh. Homaeigohar, K. Buhr, K. Ebert, *J. Membr. Sci.* **2010**, *365*, 68.
[29] D. Aussawasathien, C. Teerawattananon, A. Vongachariya, *J. Membr. Sci.* **2008**, *315*, 11.
[30] R. Gopal, S. Kaur, Z. W. Ma, C. Chan, S. Ramakrishna, T. Matsuura, *J. Membr. Sci.* **2006**, *281*, 581.
[31] R. Gopal, S. Kaur, C. Y. Feng, C. Chan, S. Ramakrishna, S. Tabe, T. Matsuura, *J. Membr. Sci.* **2007**, *289*, 210.
[32] T. Godjevargova, V. Konsulov, A. Dimov, *J. Membr. Sci.* **1999**, *152*, 235.
[33] T. Dai, N. Miletic, K. Loos, M. Elbahri, V. Abetz, *Macromol. Chem. Phys.* **2010**, *212*, 319.
[34] M. Gonzalez, P. Kadlec, P. Spepanek, A. Strachota, L. Matejka, *Polymer* **2004**, *45*, 5533.
[35] J. Gonzalez-Benito, *J. Colloid Interface Sci.* **2003**, *267*, 326.
[36] A. Romo-Uribe, L. Arizmendi, M. E. Romero-Guzman, S. Sepulveda-Guzman, R. Cruz-Silvan, *ACS Appl. Mater. Interfaces* **2009**, *1*, 2502.
[37] S. Bal, *Mater. Des.* **2010**, *31*, 2406.
[38] S. Sh. Homaeigohar, M. Elbahri, *J. Colloid Interface Sci.* **2012**, *372*, 6.
[39] D. Zhang, O. Neumann, H. Wang, V. M. Yuwono, A. Barhoumi, M. Perham, J. D. Hartgerink, P. Wittung-Stafshede, N. J. Halas, *Nano Lett.* **2009**, *9*, 666.
[40] E. G. Ferrer, A. Bosch, O. Yantorno, E. J. Baran, *Bioorg. Med. Chem.* **2008**, *16*, 3878.
[41] H. El-Sherif, M. El-Masry, M. F. Abou Taleb, *J. Appl. Polym. Sci.* **2009**, *115*, 2050.
[42] D. H. Chou, C. V. Morr, *J. Am. Oil Chem. Soc.* **1979**, *56*, A53.
[43] I. Lynch, K. A. Dawson, *Nano Today* **2008**, *3*, 40.

[44] T Cedervall, I. Lynch, S Lindman, T. Berggard, E. Thulin, H. Nilsson, K. A. Dawson, S. Linse, *Proc. Natl. Acad. Sci. USA* **2007**, *104*, 2050.
[45] X. L. Kong, L. C. L. Huang, C. M. Hsu, W. H. Chen, C. C. Han, H. C. Chang, *Anal. Chem.* **2005**, *77*, 259.
[46] F. Brouers, D. Rauw, J. P. Clerc, G. Giraud, *Phys. Rev. B* **1994**, *49*, 14582.
[47] G. A. Niklasson, *J. Appl. Phys.* **1987**, *62*, 258.
[48] V. A. Markel, L. S. Muratov, M. I. Stockman, T. F. George, *Phys. Rev. B* **1991**, *43*, 8183.
[49] V. M. Shalaev, R. Botet, *Phys. Rev. B* **1994**, *50*, 12987.
[50] M. I. Stockman, L. N. Pandey, L. S. Muratov, T. F. George, *Phys. Rev. B* **1995**, *51*, 185.
[51] *Optical properties of nanostructured random media*, (Ed: V. Shalaev), Springer-Verlag, Berlin, Heidelberg **2002**.
[52] E. E. Narimanov, A. V. Kildishev, *Appl. Phys. Lett.* **2009**, *95*.
[53] A. V. Kildishev, L. J. Prokopeva, E. E. Narimanov, *Opt. Express* **2010**, *18*, 16646.
[54] Science News, in *ScienceDaily*, April 29, **2008**.
[55] H. G. Hicke, I. Lehmann, G. Malsch, M. Ulbricht, M. Becker, *J. Membr. Sci.* **2002**, *198*, 187.
[56] F. Wang, *J. Foreign Med.* **1991**, *12*, 145.
[57] S. Sh. Homaeigohar, H. Mahdavi, M. Elbahri, *J. Colloid Interface Sci.* **2012**, *366*, 51.